Development and Control of Articulated Mobile Robot for Climbing Steep Stairs

Motoyasu Tanaka, *Member, IEEE,* Mizuki Nakajima, Yosuke Suzuki, *Member, IEEE,* and Kazuo Tanaka, *Fellow, IEEE*

***Abstract*—In this work, we develop an articulated mobile robot that can climb stairs, and also move in narrow spaces and on three-dimensional terrain. The paper presents two control methods for this robot. The first is a three-dimensional steering method that is used to adapt the robot to the surrounding terrain. In this method, the robot relaxes its joints, allowing it to adapt to the terrain using its own weight, and then resumes its motion employing the follow-the-leader method. The second control method is the semiautonomous stair climbing method. In this method, the robot connects with the treads of the stairs using a body called a connecting part, and then shifts the connecting part from its head to its tail. The robot then uses the sensor information to shift the connecting part with appropriate timing. The robot can climb stairs using this method even if the stairs are steep and the sizes of the riser and the tread of the stairs are unknown. Experiments are performed to demonstrate the effectiveness of the proposed methods and the developed robot.**

***Index Terms*—Articulated mobile robot, stair climbing, terrain adaptability, search and rescue, plant inspection**

I. Introduction

ARTICULATED mobile robots have structures in which multiple segments that can generate a propulsive force are connected by joints, which allows the robots to have elongated shapes and to enter narrow spaces. In addition, such robots can operate on complex terrain because they move under the effect of propulsive forces that are generated by the segments while freely changing their body shapes via their joints. Many articulated mobile robots have been developed (see [1]) for applications such as pipe inspection [2]–[5] and search and rescue operations at disaster sites [6]–[9] because of these characteristics.

Considering the funds, operation, and maintenance, it is important how to use a rescue robot in nondisaster situations. One of the use of a rescue robot other than disaster scenarios is inspection of industrial plants. Mobility required for plant inspection robots is ascending and descending of steep stairs, and overpassing obstacles such as piping. The crawler type with flippers and leg type robots have been developed for gas and oil plants as [10]. It seems that an articulated mobile robot can make an inspection through a narrow passage which could not be passed by the other type robots because it has elongated bodies. The ultimate goal of the present study is to realize an articulated mobile robot that is capable of not only search and rescue operations at disaster sites but also inspection of industrial plants in nondisaster situations.

Stairs are an example of terrain on which it is difficult for the articulated mobile robots to move. A problem that typically arises when an articulated mobile robot climbs stairs is that a stuck state occurs for the joints and the edges of the stairs because most articulated mobile robots do not have propulsion mechanisms located in their joints. The ACM-R4.1 [11] and 4.2 [12], which are robots composed of rotary joints and active wheels that are equipped with torque sensors, can enter narrow areas because they are relatively small, but no stair climbing ability has been reported for these robots. In contrast, the KR-II [13] was able to climb stairs using large-diameter active wheels and joints that move up and down linearly. The ACM-R8 [14], which is composed of joints with a parallel link mechanism and large-diameter mono-tread wheels, was also able to climb stairs. KR-II and ACM-R8 were able to climb stairs by arranging their joints so that they did not come into contact with the terrain and used the capabilities of large-diameter wheels to overcome high obstacles.

One way to avoid the stuck state that results from contact between the joints and stairs is to reduce the proportion of the robot's joints along the body length direction while increasing the proportion of the segments that provide propulsive forces. All parts of the flexible mono-tread mobile track [15] can generate a propulsive force along the body length direction, and the track can propel the robot as a whole, including the bending part; the robot therefore can succeed in climbing both linear stairs and a spiral staircase. Another way to avoid the stuck state is the appropriate use of joint motion. The KAIRO 3 [8] robot has modules with relatively small active wheels that are connected by a three-degree-of-freedom joint that includes an oblique swivel axis. The KAIRO 3 has a three-dimensional laser sensor on its head, and autonomously climbed two steps on a staircase using a map created from three-dimensional scans. However, the staircase in this example consisted of only two steps. The OT-4 [9] robot has segments with tracks that are serially connected using two-degree-of-freedom rotary joints. The OT-4 climbed stairs that sloped at 40° when supported by a reinforcement learning system called the *7G control system* [16]. The joint motion required to avoid a stuck formation is obtained by the learning system.

In the cited studies, each robot climbed stairs while pressing a wheel or crawler against the edge of a staircase. Therefore,

This work was partially supported by JSPS KAKENHI Grant Number 26870198, and the ImPACT Program of Council for Science, Technology and Innovation (Cabinet Office, Government of Japan).

M. Tanaka, M. Nakajima, and K. Tanaka are with the Department of Mechanical Intelligent Systems Engineering, the University of Electro-Communications, Tokyo 182-8585 Japan. (e-mail: mtanaka@uec.ac.jp, phone/fax: +81-42-443-5430)

Y. Suzuki is with Kanazawa University, Kanazawa 920-1192 Japan.

Manuscript received April 19, 2005; revised August 26, 2015.

when the stairs are steep, slippage occurs and it is impossible for the robot to climb these stairs.

This work aims to realize an articulated mobile robot that is capable of not only movement in narrow spaces and three-dimensional movement for search and rescue at disaster sites but also climbing steep stairs for inspecting a plant. This paper deals with two control problems of an articulated mobile robot. One is terrain-following control on uneven terrain for search and rescue tasks. The other is stair climbing control for inspection tasks in nondisaster situation.

The contributions of this paper are as follows.

- A three-dimensional steering method that uses manual intermittent terrain adaptation is proposed. The robot adapts to the surrounding terrain by zeroing the torque of some of its joints, and it then moves while following the terrain by resuming three-dimensional motion from the posture that is suited to the terrain. The method does not require either the measurement of forces (e.g., the wheel torque and external force) or the measurement of external information (e.g., distances to obstacles). Because torque and force measurements are unnecessary, even a simple robot that is composed of a servo motor for hobby purposes can adapt to the surrounding terrain using the proposed method, and the cost of the robot can thus be reduced.
- A semiautonomous stair climbing control method that uses sensor information is proposed. A simple operation by the operator allows the robot to ascend/descend staircases with unknown height and depth parameters. The effectiveness of the proposed method does not depend on the presence or absence of a riser. The robot can climb the stairs safely, even if the stairs are steep.
- An articulated mobile robot for stair climbing is developed, the basic performance of the robot is evaluated, and the effectiveness of the proposed control method is demonstrated through use of the robot. While the robot is relatively small, it has high mobility and is able to climb a steep step sloped at 54.5° and a 1-m-high step.

The remainder of the paper is organized as follows. Section II describes the robot model used and the basic three-dimensional steering control method and a simple terrain adaptation method that is based on the FTL approach. Section III proposes a control method that enables the robot to climb up and down stairs semiautonomously. Section IV describes an articulated mobile robot that was developed to realize three-dimensional motion and stair climbing. Section V evaluates the performance of the developed robot and demonstrates the effectiveness of the proposed control method experimentally using this robot.

II. Model and Three-dimensional Steering Control

It is difficult to control articulated mobile robots because they have many degrees of freedom. Two main methods are used to control these robots [1]: *n-trailer* and *follow-the-leader*. *n-trailer*, which is used in [6], [17], is a method by which the robot's motion is calculated in order from head to tail while assuming that any segment that generates propulsion does not skid. This method is only applied to planar terrain. There is also a similar method by which the motions of all joints and wheels are calculated simultaneously using a kinematic model that is derived by assuming that any wheel mounted on the segment does not skid [18]–[22]. This method was mainly proposed for use with snake robots in which links with passive wheels are serially connected through active joints. When using this method, it is possible to consider the case that some of the robot's wheels are lifted and do not touch the ground, and it is also possible to track the trajectory of the head position and the orientation simultaneously while avoiding obstacles by switching the grounding status of the wheels, as in [18], [19]. However, only steps [20], [21] and cylindrical surfaces [22] are treated as three-dimensional terrains in this case, and a control method for more complex three-dimensional terrain has not yet been established. In contrast, the *follow-the-leader* (FTL) method used in [2], [3], [11]–[14] allows the head (leader) movement to be shifted from head to tail. Using this method, the operator can easily perform three-dimensional operations by appropriate design of the robot's head movement. In this section, we propose a simple terrain adaptation method that is based on the FTL approach.

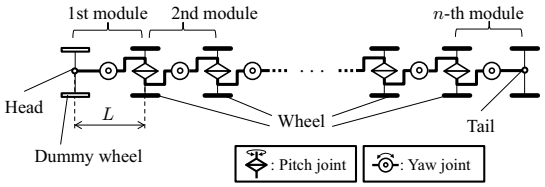

(a) An articulated mobile robot

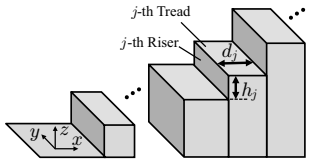

(b) Stairs

Fig. 1. Models of the robot and the stairs.

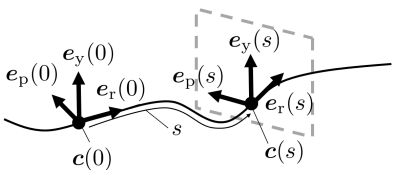

(a) Coordinates

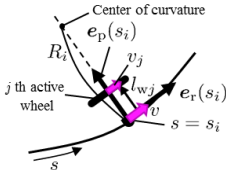

(b) Velocity of a wheel

Fig. 2. Definition of a continuous backbone curve.

A. Model

Figure 1(a) shows the model of the articulated mobile robot. The joint uses a configuration in which the yaw rotational joint and the pitch rotational joint are connected alternately in series and wheels are mounted on the left and right sides coaxially with respect to the pitch joint. This is the same joint configuration that was used in the ACM-R4.2 [12], and allows various types of motion control; e.g., control for moving-obstacle avoidance [18], whole-body collision avoidance [19], step climbing [20], [21], and stair climbing [23]. The robot can be propelled by rotating the wheels while simultaneously varying the body shape using the pitch and yaw joints. Dummy wheels with low friction and easy side slip are attached at the head of the robot. The purpose of these wheels is to simplify stair climbing control by maintaining a constant distance between the head and tread surface when the robot climbs a stair. Let l be the link length, $L = 2l$ be the module length, r be the wheel radius, ϕ_i be the angle of the i-th yaw joint, and ψ_i be the angle of the i-th pitch joint, and assume that the number of modules n is sufficiently large.

B. Shape fitting using the backbone curve

We use the shape fitting method that was proposed by Yamada et al. [11], [33] for basic three-dimensional steering of the robot because the curve representation in their method is intuitive and suitable for a robot that has the joint configuration shown in Fig. 1(a); additionally, the method has low computational cost for calculation of the target angles of the joints. A differential equation is introduced as a continuous backbone curve to express the target robot body shape:

$$\begin{cases} \frac{\mathrm{d}\boldsymbol{c}(s)}{\mathrm{d}s} & = \boldsymbol{e}_{\mathrm{r}}(s), \\ \frac{\mathrm{d}\boldsymbol{e}_{\mathrm{r}}(s)}{\mathrm{d}s} & = \kappa_{\mathrm{y}}(s)\boldsymbol{e}_{\mathrm{p}}(s) - \kappa_{\mathrm{p}}(s)\boldsymbol{e}_{\mathrm{y}}(s), \\ \frac{\mathrm{d}\boldsymbol{e}_{\mathrm{p}}(s)}{\mathrm{d}s} & = -\kappa_{\mathrm{y}}(s)\boldsymbol{e}_{\mathrm{r}}(s), \\ \frac{\mathrm{d}\boldsymbol{e}_{\mathrm{y}}(s)}{\mathrm{d}s} & = \kappa_{\mathrm{p}}(s)\boldsymbol{e}_{\mathrm{r}}(s), \end{cases} \tag{1}$$

where $\boldsymbol{c} = [x(s), y(s), z(s)]^{\mathrm{T}}$ is a vector that represents the coordinates of the continuous curve, and s is the length variable along the curve as shown in Fig. 2(a). $(\boldsymbol{e}_{\mathrm{r}}(s), \boldsymbol{e}_{\mathrm{p}}(s), \boldsymbol{e}_{\mathrm{y}}(s))$ is the backbone curve reference set that is used as the orthogonal coordinate system, $\boldsymbol{e}_{\mathrm{r}}(s)$ is a tangential unit vector for the curve at s, and $\boldsymbol{e}_{\mathrm{p}}(s)$ and $\boldsymbol{e}_{\mathrm{y}}(s)$ are unit vectors that are oriented along the pitch axis and the yaw axis, respectively. $\kappa_{\mathrm{p}}(s)$ and $\kappa_{\mathrm{y}}(s)$ are the curvatures around the pitch axis and the yaw axis in the curve reference set, respectively. $\kappa_{\mathrm{p}}(s)$ and $\kappa_{\mathrm{y}}(s)$ are parameters that are determined by the operator. $s = s_h$ is the position of the head of the robot on the curve, and the tail is located at $s = s_h - nL$.

The robot joint angles ϕ_i and ψ_i can be obtained approximately using κ_{y} and κ_{p}:

$$\begin{aligned} \phi_i &= -\int_{s_{\mathrm{h}}-2il}^{s_{\mathrm{h}}-2(i-1)l} \kappa_{\mathrm{y}}(s)\ \mathrm{d}s, \\ \psi_i &= -\int_{s_{\mathrm{h}}-(2i+1)l}^{s_{\mathrm{h}}-(2i-1)l} \kappa_{\mathrm{p}}(s)\ \mathrm{d}s. \end{aligned} \tag{2}$$

Note that the sign of (2) is different from that in [11], [33] because the beginning and end positions of the curves are different. By varying s_{h}, the area of the robot body on the curve changes, and FTL-type control is performed along the continuous curve.

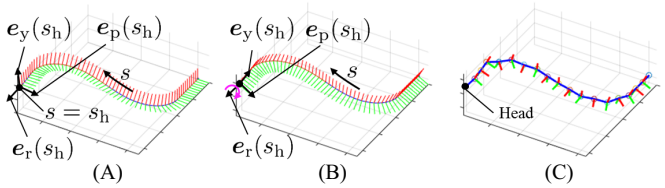

(a) Shape fitting method. (A) Target continuous backbone curve; (B) target continuous backbone curve after lateral rolling; (C) robot posture calculated using (2). In (C), red lines depict the rotational axis vectors for each joint.

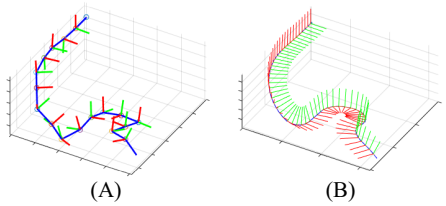

(b) Robot posture and continuous curve used in terrain adaptation. (A) Posture of the robot; (B) target continuous curve calculated using (5).

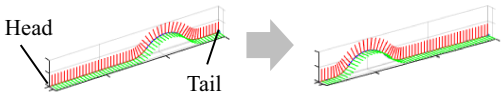

(c) Continuous curve used in recovery motion from a stuck state.

Fig. 3. Continuous target curve and robot posture.

Additionally, the robot can perform a lateral rolling motion by rotating $\kappa_{\mathrm{p}}(s)$ and $\kappa_{\mathrm{y}}(s)$ uniformly around $\boldsymbol{e}_{\mathrm{r}}$ for the entire curve. Let Ψ be the rotational angle around $\boldsymbol{e}_{\mathrm{r}}$. $\kappa_{\mathrm{p}}(s)$ and $\kappa_{\mathrm{y}}(s)$ can then be calculated as

$$\begin{bmatrix} \kappa_{\mathrm{y}}(s) \\ \kappa_{\mathrm{p}}(s) \end{bmatrix} = \begin{bmatrix} \cos\Psi & -\sin\Psi \\ \sin\Psi & \cos\Psi \end{bmatrix} \begin{bmatrix} \kappa'_{\mathrm{y}}(s) \\ \kappa'_{\mathrm{p}}(s) \end{bmatrix}, \tag{3}$$

where $\kappa'_{\mathrm{p}}(s)$ and $\kappa'_{\mathrm{y}}(s)$ represent $\kappa_{\mathrm{p}}(s)$ and $\kappa_{\mathrm{y}}(s)$ before the rolling motion, respectively. The robot can perform lateral rolling motion when the operator changes Ψ as in Fig. 3(a).

C. Design of wheel velocities

The wheel is located at a position that has deviated from the target continuous curve. Let us define the wheel velocity as $\mathrm{d}s_{\mathrm{h}}/\mathrm{d}t = v$. It is then necessary to correct the velocity of the active wheel by considering the offset caused by the curve and the curvature of the continuous curve. Let v_j be the translational velocity of the j-th active wheel when mounted coaxially with the i-th pitch joint, $s = s_i$ be the position of the i-th pitch joint located on the target continuous curve, and $l_{\mathrm{w}j}$ be the offset length between $\boldsymbol{c}(s_i)$ and the center of the j-th active wheel. For the continuous curve, $\boldsymbol{e}_{\mathrm{p}}$ and the axle of the wheels are located on the same straight line. As shown in

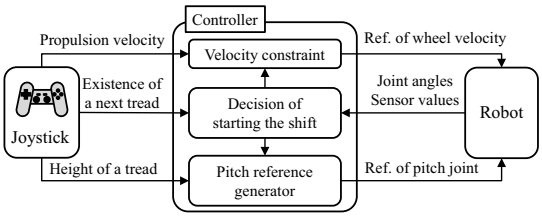

Fig. 4. Control diagram of the semiautonomous stair climbing process.

Fig. 2(b), if $\kappa_{\rm y}(s_i) \neq 0$, then the distance to the center of the curvature at $s = s_i$ is $R_i = \frac{1}{\kappa_{\rm y}(s_i)}$ on the plane that is defined by $\boldsymbol{e}_{\rm r}(s_i)$ and $\boldsymbol{e}_{\rm p}(s_i)$. Therefore, according to the geometric relation shown in Fig. 2(b), v_j can be obtained as

$$v_j = \frac{(R_i - l_{{\rm w}j})}{R_i} v. \tag{4}$$

D. Steering method

The operator first varies the continuous curve at the head of the robot by manipulating $\kappa_{\rm y}$ and $\kappa_{\rm p}$ in the region of the head. FTL-type control is then performed by varying the position of the robot along the continuous curve; i.e., by changing v, which is the velocity of $s_{\rm h}$. In addition, it is possible to perform a lateral rolling motion by varying Ψ. In this case, the operator changes Ψ, $\kappa_{\rm p}$ and $\kappa_{\rm y}$ are calculated using (3), and the target joint angles for the lateral rolling motion are calculated using (2). The active wheel rotation speed is then calculated using (4). Therefore, three-dimensional steering of the robot can be realized by controlling $\kappa_{\rm p}$, $\kappa_{\rm y}$, v, and Ψ.

E. Terrain-following by manual intermittent adaptation

To move across complex terrain, a robot requires operating modes such as terrain following, obstacle avoidance, and utilization (pushing) of obstacles. Considerable research into these operations has been carried out on both articulated mobile robots and snake-like robots without wheels. On a two-dimensional plane, adaptation to obstacles based on the contact force with these obstacles [24], obstacle-aided locomotion [25]–[27], and obstacle avoidance based on distance sensor information [19], [28] have all been proposed. Motion inside and outside a pipe, adaptation to changes in pipe diameter [29] and bent pipes [30] through pipe diameter estimation using an extended Kalman filter, and motion on a horizontal pipe using a passive compliant element to adapt to flange and pipe diameter changes [31] have been proposed. On complex three-dimensional terrain, adaptation to the terrain using a torque sensor-based method [11], [32] has been proposed. If all the following parts of the robot can continue along the path of the head of the robot when using FTL-type control, the robot can move forward, even across complex three-dimensional terrain. However, in practice, wheel slip and changes in the contact position between the robot and terrain cause the following parts to travel along a path that differs from that of the head. This causes problems, including unintentional contact with the terrain resulting in a stuck state and excessive loading of the joints, and may even cause the robot to fall. By adapting to the terrain in the manner of [11], [32], the robot can reduce joint loading and prevent itself from falling.

This paper proposes a simple terrain adaptation method that does not require either measurement of forces, e.g., the wheel torque and the external force, or measurement of external information, e.g., distances to obstacles. Because torque and force measurements are unnecessary, even a simple robot that is composed of a servo motor for hobby purposes can adapt to the surrounding terrain using the proposed method, and the cost of the robot can thus be reduced. In this method, the robot makes the torque at the joint zero, and adjusts its shape to that of the terrain using its own weight. The problem to be solved here is how to calculate the continuous curve $\boldsymbol{c}$ after the terrain adaptation process. FTL operation is performed using the joint angle, which is calculated from the continuous curve $\boldsymbol{c}$. When the torque at the joint is set to zero, the joint angle changes because of the interaction with the terrain, and the entire continuous curve must be recalculated from the perspective of the current angle. Because determination of a continuous curve from discrete angle information is an inverse problem, the solution is not determined uniquely. We therefore assume that the curvature $\kappa_{\rm y}(s)$ at $s_{\rm h} - 2il < s \leq s_{\rm h} - 2(i-1)l$ and the curvature $\kappa_{\rm p}(s)$ at $s_{\rm h} - (2i+1)l < s \leq s_{\rm h} - (2i-1)l$ are the constant values $\kappa_{{\rm y}i}$ and $\kappa_{{\rm p}i}$, respectively. From (2), $\kappa_{{\rm y}i}$ and $\kappa_{{\rm p}i}$ can then be calculated as

$$\kappa_{{\rm y}i} = -\frac{\phi_i}{2l}, \quad \kappa_{{\rm p}i} = -\frac{\psi_i}{2l}. \tag{5}$$

The curvatures $\kappa_{\rm y}(s)$ and $\kappa_{\rm p}(s)$ can be obtained by calculating (5) for all joints, and the robot can then restart FTL operation based on the adapted body shape after terrain adaptation. An example is shown in Fig. 3(b). It is thus considered that the robot can respond flexibly to complex terrain by simply varying the timing and the corresponding joints when the operator sets the torque to zero, depending on the specific situation. Note that there are fall risks that depend on the choice of joint when the torque is set to zero if there are few contact points between the robot and terrain (e.g., when overcoming a valley).

F. Recovery motion from a stuck state

If the terrain is not smooth, the joint parts of the robot may become stuck even if the robot uses the terrain-following method. Thus, a traveling wave motion of the pitch angles is used as a recovery motion from a stuck state. In the motion, a traveling wave moving from the tail to the head is prepared on $\kappa_{\rm p}$ as in Fig. 3(c), and the robot moves using a curve obtained by overlaying a traveling wave on the original continuous backbone curve. If the traveling wave reaches the stuck part of the body, the stuck part separates from the terrain and the robot recovers from the stuck state.

III. Semiautonomous Stair Climbing

The stairs shown in Fig. 1(b) are assumed to be the environment. Let h_j be the height of the j-th riser and let d_j be the depth of the j-th tread. It is assumed that the robot can detect contact between each pair of wheels and the stair tread surface using sensors that are mounted on the robot.

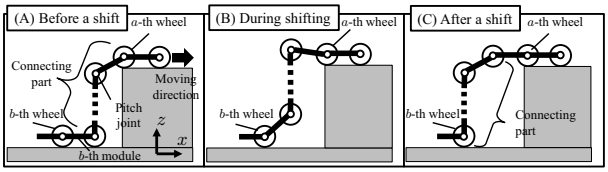

(a) Climbing up the stairs

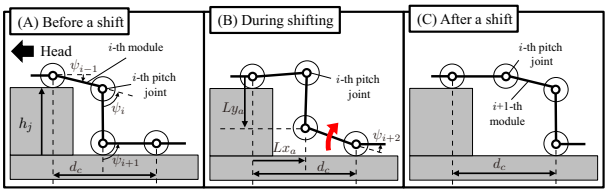

(b) Climbing up the stairs (two modules)

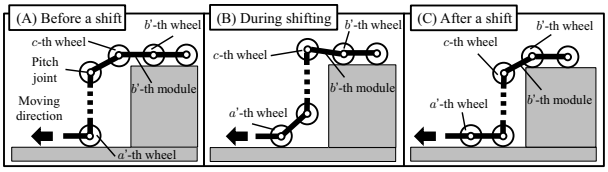

(c) Climbing down the stairs

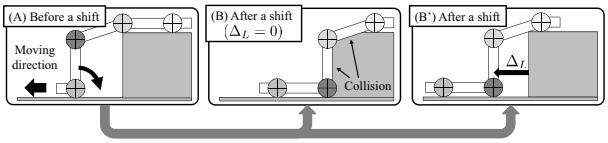

(d) Shift with Δ_L in climbing down stairs

Fig. 5. Shift in the connecting part.

A sufficiently large value of d_j with respect to L makes the motion planning process easier because the area in which the robot can move is then wider. In contrast, if d_j is small, then the area for the robot is small. In this case, few wheels are touching the tread and the risk of the robot falling increases when some of these wheels fall from the tread. In addition, the body of the robot cannot move far from the riser because d_j is small. It is thus difficult for the robot to climb the stairs while avoiding collisions between the robot and stairs. We previously proposed a stair climbing method for the case that d_j is relatively small in [23]. However, this method assumes that the size of the rise/tread of the stairs is known, and the operator must therefore check the relative relationship between the robot and stairs from a bird's-eye viewpoint and give commands at appropriate times. This situation is unrealistic and impractical.

The present paper proposes a control method for an articulated mobile robot on stairs with unknown riser and tread parameters that improves on the previous method [23].

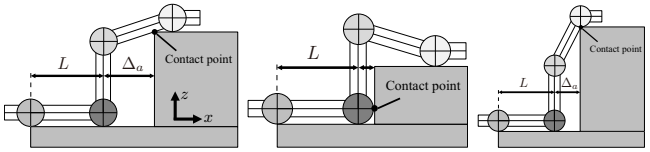

(a) (b) (c)

Fig. 6. Δ_a and the connecting part (two modules) for (a) $\Delta_a > r$, (b) $\Delta_a = r$, and (c) the highest riser. If the riser is higher than that shown in (c), then wheel a cannot be in contact with the tread because of contact between the body of the robot and the tread.

Assuming that remote control is used, a camera is normally installed at the head of the robot. Even when the height of the rise is unknown, it is possible to adjust the height to an extent by operating the robot on the basis of the camera images and sensor information. It is therefore assumed that the operator sets the rise height manually using the sensor information. In contrast, if the depth of the tread is unknown, it then becomes difficult for the operator to operate the robot. This is because it is difficult for the operator to recognize the tread depth and to measure the depth using a sensor (e.g., a distance sensor) when there is no riser surface present. In the proposed method, the operator does not need to consider the tread depth and can operate the robot by focusing on the head alone, because the robot moves semiautonomously according to sensor information from the body part.

Figure 4 shows the control diagram for the proposed method. The operator provides the robot with the following three control commands using a joystick.

- The propulsion velocity
- The decision on whether or not the next stage exists
- Adjustment of the estimated height of the next riser that the head is approaching

In the *pitch reference generator*, the target pitch joint angle is calculated employing the method described in section III-A and is then output to the robot. In the *start condition for the shift*, the decision to start the shift that is related to the target pitch angle is made according to the conditions that are described in section III-B. In *velocity constraint*, a velocity constraint is determined following section III-D, and the target wheel speed is determined. The case of climbing up stairs is described first in this section while the case of climbing down stairs is described in section III-E.

A. Shift in the connecting part [23]

In [23], the *connecting part*, which is the module of the robot that connects the two treads, was introduced and the robot climbed up stairs by shifting the connecting part from its head to its tail. If the robot uses the shift in the connecting part, then the yaw angle of the connecting part must be zero, as per [20], [23]. The yaw angle thus cannot be used to steer the robot. In the case that d_j is small, almost all modules become a connecting part having a zero yaw angle and the robot thus cannot use the yaw angles for steering purposes.

We proposed a straight stair climbing method without steering in [23] while assuming that d_j was small. The state of the shift in the connecting part from [23] is shown in Fig. 5(a). By maintaining a constant relative distance between the a-th wheel and the b-th wheel, the robot can prevent these wheels from falling out of the tread during the shift because the following part of the connecting part will not travel backwards. When using this method, the robot cannot steer when climbing up and down the stairs, but it can at least climb the narrow stairs.

Here, we consider the case that the connecting part consists of two modules. Figure 5(b) depicts the shift in the connecting part in the case of climbing up the stairs. The i-th and $i+1$-th modules represent the connecting part before the shift. After the shift, the connecting part is represented by the $i+1$-th and $i+2$-th modules. The connecting part connects the j-th and $j-1$-th treads, and we also define $L \leq h_j \leq 2L$ here. Let the start time of the shift be t_{st} and the end time of the shift be $t_{st}+t_\psi$. We set x_a and y_a as

$$x_a = (d_c - L\cos\psi_{i+2})/L,\ y_a = (L\sin\psi_{i+2} - h_j)/L. \quad (6)$$

From Fig. 5(b), the geometric relationships are

$$d_c = L + \sqrt{L^2 - (h_j - L)^2}, \quad (7)$$

$$Lx_a = -L\{\sin\psi_{i-1} + \sin(\psi_{i-1}+\psi_i)\}, \quad (8)$$

$$Ly_a = L\{\cos\psi_{i-1} + \cos(\psi_{i-1}+\psi_i)\}. \quad (9)$$

From (7)–(9), we set the motions of the pitch joints $\psi_{i-1}, \cdots, \psi_{i+2}$ as

$$\left.\begin{array}{ll} \psi_{i+2} & = \frac{\pi}{2}t' \\ \psi_i & = -\cos^{-1}\frac{x_a^2+y_a^2-2}{2} \\ \psi_{i-1} & = \mathrm{atan2}(y_a, x_a) + \cos^{-1}\frac{\sqrt{x_a^2+y_a^2}}{2} \\ \psi_{i+1} & = -\psi_{i-2} - \psi_{i-1} - \psi_i, \end{array}\right\} \quad (10)$$

where t is time, $t' = 6\tilde{t}^5 - 15\tilde{t}^4 + 10\tilde{t}^3$ is the fifth-dimensional curve given as a cam curve, $\tilde{t} = \frac{t-t_{st}}{t_\psi}$, and $t_{st} \leq t \leq t_{st} + t_\psi$. The robot can maintain a constant value of d_c, which is shown in Fig. 5(b), using (10). The shape of the connecting part can be determined freely as long as the relative distance d_c between the a-th and b-th wheels shown in Fig. 5(a) remains constant.

B. Start condition for the shift

It is assumed here that the robot does not move backwards when climbing up and down the stairs. The robot can determine whether or not each wheel axle is contacting the tread surface using the mounted sensor. The starting conditions for the shift process are designed as follows.

1) The b-th module is not a connecting part.
2) The a-th and b-th wheels are located on the tread surface.

Condition 1 guarantees that the b-th module is ready to be shifted. Condition 2 is necessary to maintain the static stability of the connecting part before and after the shifting process. If condition 2 is satisfied, then the connecting part is supported by the a-th and b-th wheels both during and after shifting. If the module that is included in the connecting part collides with the stairs before the a-th wheel touches the tread surface, conditions 1 and 2 cannot be used. The available solutions in that case involve either improving the shape of the connecting part or using the $(a-1)$-th wheel rather than the a-th wheel for condition 2 in Fig. 5(a).

C. Geometric conditions of stairs

The geometrical conditions that the stairs must satisfy when the robot climbs the stairs based on the starting conditions described in the previous subsection are described below. As shown in Fig. 6, we let Δ_a be the distance between the contact point and the rear end module of the connecting part in the x direction as the robot moves forward until the robot and stair make contact. To satisfy condition 2, the $(j-1)$-th tread must satisfy the condition

$$d_{j-1} \geq L + \Delta_a, \quad (11)$$

where Δ_a depends not only on the riser height but also on the module length L and the link geometry of the robot.

D. Velocity constraint

If the robot moves forward appreciably during the shift, there may be a collision between the robot and stairs. It is thus desirable that the forward motion of the robot be restricted as much as possible during the shift process. However, there are cases where the wheel is determined to exist on the tread surface before it actually touches the tread surface as a result of the inaccuracy and noise error of the sensor used. In addition, because of wheel slippage, the wheels (i.e., the a-th and b-th wheels in Fig. 5(a)) that should support the connecting part during the shift may move backwards and may then fall off the tread in some cases. In such cases, if the robot does not move forward, there is then the possibility that the balance will be lost during the shift. To solve these problems, the robot moves forward by a specific distance during each shift. Let Δ_L be the distance by which the robot moves forward during the shift. The forward velocity v during the shift can then be designed as

$$v = \Delta_L / t_\psi. \quad (12)$$

E. Climbing down the stairs

Figure 5(c) depicts the shift in the connecting part when climbing down the stairs. The motion is similar to a reverse playback of the process of climbing up the stairs. The specific equation for the joint angle is omitted, and differences from the case of climbing up the stairs are described. The start conditions for climbing down the stairs are designed as follows.

1) The b'-th module is not the connecting part.
2) The a'-th and b'-th wheels are located on the tread surface.
3) The c-th wheel is not contacting the tread surface.

Conditions 1 and 2 here correspond to conditions 1 and 2 of Section III-B, respectively. Condition 3 represents the trigger

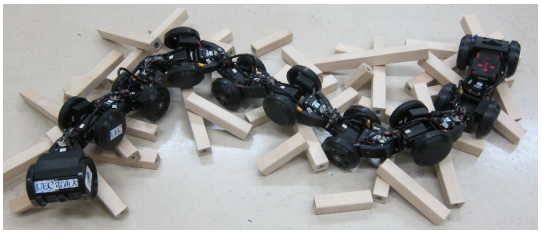

(a) Overall view

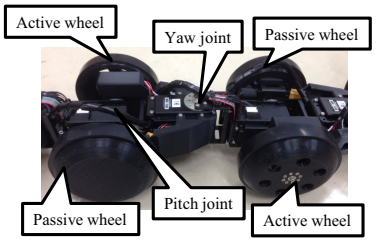

(b) Enlarged view

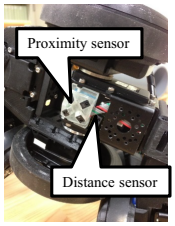

(c) Bottom view

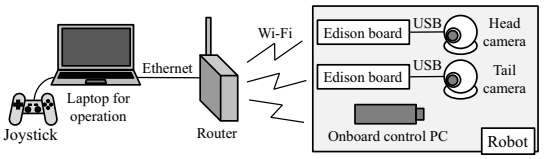

(d) Complete system

Fig. 7. Articulated mobile robot *T*^{2} *Snake-3*.

for the start of the shift process. In climbing down the stairs, if the robot shifts with $\Delta_L = 0$ in (12), then the connecting part may contact the tread as shown in (B) in Fig 5(d). In this case, the robot must move forward during the shift using an appropriate value of Δ_L, as shown in (B') in Fig. 5(d). The appropriate Δ_L depends on the wheel diameter, the riser height, and the link geometry of the robot.

If the b'-th and c-th wheels are changed to the $(b'+1)$-th and $(c+1)$-th wheels, respectively, the robot can then shift the connecting part without collision with $\Delta_L = 0$, but the required tread depth for the shift is increased. To match the required tread depths of the stair when climbing up and down, it is necessary to use the grounding and ungrounding of the c-th wheel, as shown in Fig. 5(c), as the trigger for the shift when climbing down the stairs.

IV. Development of an Articulated Mobile Robot

Figure 7 depicts the developed robot, which is called *T*^{2} *Snake-3* and has the parameters given in Table I. The robot is battery powered and can be controlled remotely on a wireless basis.

TABLE I
PARAMETERS OF THE ARTICULATED MOBILE ROBOT.

Number of modules n	9
Link length l [mm]	90.5
Module length L [mm]	181
Total size (H × W × L) [mm]	120×150×1729
Wheel radius r [mm]	50
Joint angle range (Pitch) [deg.]	$\lvert\psi_i\rvert \leq 113$
Joint angle range (Yaw) [deg.]	$\lvert\phi_i\rvert \leq 65$
Total mass [kg]	9.2
Battery life [min.]	about 80

A. Mechanical Design

The joint configuration of the robot is the same as that of the model shown in Section II. Dynamixel servos (ROBOTIS Inc.) are used as actuators for both the joints and active wheels. MX-106R and MX-28AR models are used for the joints and wheels, respectively. To enable stair climbing when using the proposed method, the robot must have a wide pitch joint angle range that exceeds $\pm 90°$, as in [23]. The range of the pitch joint angle is therefore designed to be as wide as possible.

In the stair climbing case using the proposed method, the robot must have active wheels to be propelled because it does not undulate laterally in the manner of a snake robot, such as that of [24]. Additionally, the contact and noncontact conditions between the wheels and the tread surface change frequently. If at least one wheel on each axle is an active wheel, the robot can then generate propulsion because there are always wheels in contact with the tread. Therefore, one wheel on each axle is the active wheel while the other wheel is a passive wheel, as shown in Fig. 7(b). The wheels are active on both sides at the tail axle only. The mounting of these passive wheels is intended to reduce the overall size of the robot. The passive wheels are structured so that only the outer ring of each wheel rotates, and space for a battery is provided inside the passive wheel.

At the head and tail of the robot, cameras that obtain images, Intel Edison Modules that acquire these camera images and transmit them wirelessly, and batteries are installed. At the tail, an Intel Compute Stick is installed to act as the onboard control personal computer (PC) for the robot.

The robot has an infrared distance sensor and a proximity sensor [34] located at the bottom of its body to measure the distance and inclination angle between the robot and surrounding plane, as shown in Fig. 7(c). The robot can determine whether the wheel makes contact with the ground according to distance information with respect to the tread surface during stair climbing. Specifically, the contact between each pair of wheels and the stair tread surface is detected by comparing the distance information measured by the sensor with the threshold value.

B. Communication system design

The communication system that connects the onboard control PC, actuators, and sensors comprises a master microcontroller unit (MCU) and multiple slave MCUs, and the actuators and sensors are connected to each of the slave MCUs. A

TABLE II
BASIC MOBILITY PROPERTIES OF THE PROPOSED ROBOT.

Propulsion speed [mm/s]	250
Maximum trench width [mm]	550
Maximum step height without riser [mm]	675
Maximum step height with riser [mm]	1030
Minimum width of L-shaped path [mm]	250

SEED-MS1A (THK Co., Ltd.) is used as the MCU in this case. Communications are made between the master MCU and slave MCUs via a controller area network, while those between the master MCU and the control PC use an RS-485 system. The master MCU sends commands from the control PC to each slave MCU, collects data from the actuators and sensors that are connected to each slave MCU, and sends the resulting data to the control PC. Each slave MCU communicates with the corresponding actuator and reads the sensor data according to commands from the master MCU, and transmits the acquired data to the master MCU. During communications with the actuator, the slave MCU transmits the target angle and target speed, and receives the joint angle, current, and error information in return.

C. Complete system

Figure 7(d) shows the complete system. The laptop used for system operation, the onboard control PC, and the Edison boards are all connected to the same network, which is managed by a router. The operator sends commands to the robot using a joystick. The operating system of the laptop for system operation is Ubuntu 14.04, and it acquires the joystick information via the robot operating system (ROS) and transmits this information to the control PC. The control PC then controls the robot by calculating the control inputs based on the operator's commands. The control PC uses the Windows 10 operating system, and the control PC uses Matlab 2015b with the Robotics System Toolbox to control the robot and to communicate with the ROS network. Robot information (e.g., joint angle) acquired by the control PC is then transmitted to the operator's PC via the network.

V. EXPERIMENT

A. Basic performance using FTL control

The basic performance characteristics of the proposed robot are given in Table II. During the performance evaluation experiment, the method described in Section II was used to steer the robot, and the operator provided steering commands while looking at the robot itself rather than a camera image. The status of the experiments is illustrated in Fig. 8. While there are incomplete numbers in Table II because of the limitations of the experimental environment, the maximum sizes of both a trench and a step and the minimum size of an L-shaped path in Table II are the highest performance values that were obtained from the experiments, which were performed with increments of 50 mm. In the case of climbing a step with a riser, the wheels of the robot that were in contact with the riser surface not only generated propulsion but also reduced the load on the pitch joint, and it was possible to suppress tendencies to fall backward. As a result, the robot was able to climb to a higher step when compared with the case of climbing a step without a riser surface. This performance means that the robot can climb onto a typical desk if there is a riser surface available. Table III compares the

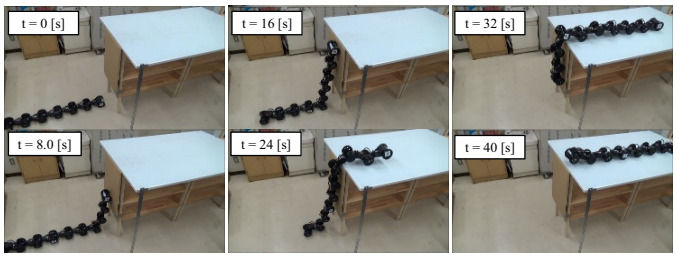

(a) Climbing a step with a riser (height: 1030 mm).

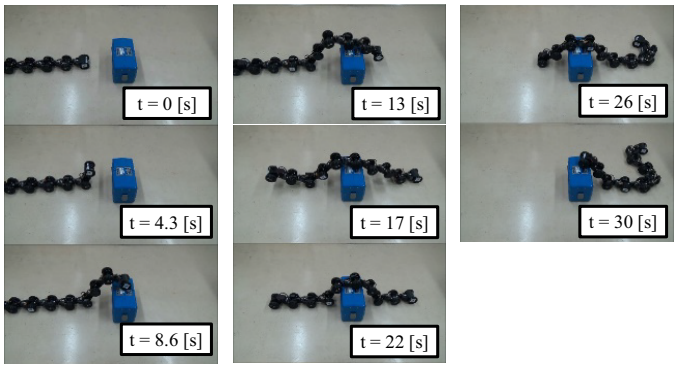

(b) Climbing a box using the proposed method.

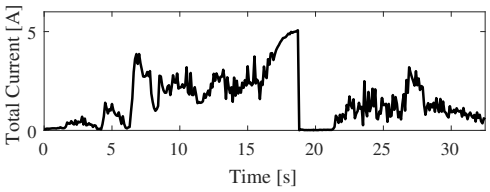

(c) Summation of the absolute value of the current of the joint when climbing a box.

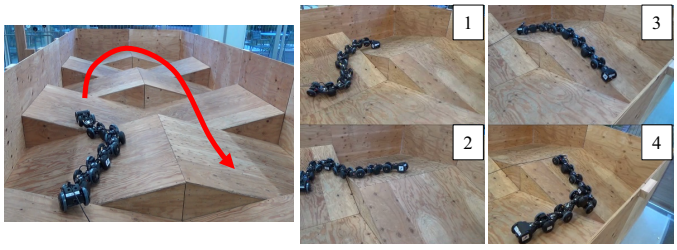

(d) Crossing ramps [35].

Fig. 8. Photographs of the experiments.

step climbing performances of snake-like articulated mobile robots. The table shows that the proposed robot has a high step climbing performance. Even when the total length of the robot is considered, the performance of the proposed robot exceeds that of the rescue robot Soryu V [7], which has three crawler units that are serially connected by joints.

As a demonstration of the terrain-following performance achieved by manual intermittent adaptation, an operation to climb over a tool box with a height of 0.24 m was performed as shown in Fig. 8(b). The operator observed the robot motion visually and provided a command to steer the head and zero the torque. The joints at which the torque was zeroed are all pitch joints. The operator then applied a manual adaptation using the proposed method between $t = 17$ s and $t = 22$ s. At $t = 17$ s, many of the parts of the robot were lifted off the ground, and a heavy load was thus applied to the joints. In contrast, the body posture at $t = 22$ s was improved by the terrain adaptation procedure. From Fig. 8(c), the summation of the absolute value of the current of the joint decreased greatly to almost zero at the time of manual adaptation. After the robot adapted to the terrain, FTL operation resumed and the robot was able to climb over the box. Moreover, the robot was able to pass through a field of crossing ramps [35] using the proposed terrain-following method as shown in Fig. 8(d). In the field, there were cases that the joint was stuck after terrain-following, but the robot was able to recover from the stuck state by performing the traveling wave motion of the pitch angles described in section II-F.

Note that the operation is performed manually, and the results thus depend on the skill of the operator. Establishment of an autonomous or semiautonomous control method that is independent of the skill of the operator will be a subject of future work.

B. Semiautonomous stair climbing

The operator is only required to adjust the height of the foremost connecting part because the robot shifts this part from its head to its tail. The operator then adjusts the height while confirming the inclination outputs of both the proximity sensor and the distance sensor that are attached to the bottom of the robot's body. A constant distance between the center of the dummy wheel and the tread surface is maintained by pressing the dummy wheel against the tread surface. Thus, a distance between the center of the head and the tread surface is maintained constant.

Figures 9(a) and 9(b) show how the robot climbed up and down stairs that were composed of risers and treads with various heights and depths. The operator manually adjusted the height of the robot's head while looking at the sensor value, and then moved the robot forward. The robot started the shift in the connecting part at an appropriate time based on the available sensor information. As a result, the robot was able to ascend and descend stairs without becoming stuck.

If condition (11) is satisfied, the robot will also be able to climb steep stairs using the proposed method. Figure 9(c) depicts the case of climbing steep stairs that were sloped at 54.5°, and which the other articulated mobile robots cannot climb, as shown in Table III. If the number of modules that make up the connecting part is increased, the robot can then climb even steeper stairs. However, it is noted that there are limits to the number of modules that can be used for the connecting part that depend on the actuator torque. Additionally, the parameters of the steep stairs used in this experiment do not conform to the ISO 14122-3 standard [36]. However, because the conditions for stair climbing when using the proposed method have been clarified in the above section, if the module length L of the robot can be reduced, then the robot will be able to climb steep stairs that satisfy the ISO standard.

Figure 9(d) shows an experiment that was conducted on stairs at the University of Electro-Communications, Tokyo, Japan. On these stairs, the robot changed its target angle using the method described in Appendix A because the target angle exceeded the limit value given in Table I. The riser height is the same for all stairs and the operator only had to adjust the riser height for the first stair. The robot was able to climb up 10 steps of these stairs in 205 s because the height adjustment was only required once and the adjustment time was short.

We then considered the case that the robot moved on stairs in an oblique direction that was not parallel to x in the xy plane. If the stair width is low, there is a risk that the robot will fall towards the side of the stairs or will collide with a wall at the side of the stairs because the robot cannot be steered using the proposed stair climbing method. It is thus desirable that the robot enters the stairs in parallel with the x axis direction as much as possible. For example, if the posture of the robot before it climbs a stair is changed appropriately using the method of [37], the risks of falling and collision with a wall can be reduced.

If the robot can detect the height of the stair with a laser range sensor mounted at the head of the robot as in [21], it seems that the robot will be able to automatically ascend and descend stairs without an operator, which is a topic of future work.

The stair climbing method can also be applied to allow the robot to enter a horizontal pipe, as shown in Fig. 9(e). The distance between the ground plane and the inner wall of the pipe is 180 mm. In the case that the robot enters the pipe using the FTL method, it is possible that the joint part of the robot will collide with the pipe because the following part of the robot may pass along a path that differs greatly from that followed by the robot's head owing to slippage of the wheel. In contrast, in the case that the stair climbing method is used, even if there is slippage of the wheel, the robot can still enter the pipe because the robot can shift the connecting part at an appropriate time according to sensor information.

VI. CONCLUSION

With the aim of realizing an articulated mobile robot that is capable of not only movement for search and rescue at disaster sites but also climbing steep stairs for inspecting industrial plants, this paper presented a basic three-dimensional steering method with terrain following based on intermittent manual adaptation and a semiautonomous stair climbing method that

TABLE III
COMPARISON OF STEP CLIMBING PERFORMANCES OF ARTICULATED MOBILE ROBOTS.

Feature \ Robot	T^2 Snake-3	Soryu V [7]	OT-4 [9]	RT04-NAGA [15]	ACM-R4.2 [12]	ACM-R8 [14]
Total length [mm]	1729	1160	940	1255	983	2010
Maximum step height with riser [mm]	1030	640	400	500	370	600
[%] of robot length	60	55	43	40	38	30
Maximum degree stairway [deg.]	54.5	–	40	40	–	30
(Rise/Tread) [mm]	(350/250)	–	–	(200/240)	–	(150/260)

uses sensor information. An articulated mobile robot was then developed, and the effectiveness of the proposed control method was demonstrated experimentally. The developed robot can move along a narrow path using its elongated body, adapt to the surrounding terrain, climb a 1-m-high step, and climb steep stairs. On the basis of these characteristics, the robot will be able to enter and overcome many different terrains, and it is likely to be useful for the inspection of houses and industrial plants.

Future work will involve the proposal of a control method that assumes use on terrains such as a spiral staircase, the interior and exterior of a pipe, and rubble, with the aim of expanding the range of terrain through which the robot can move.

APPENDIX A
JOINT LIMIT AVOIDANCE

When the rotation angle required for shifting the connecting part exceeds the robot's limit angle, it is necessary to modify the shift motion. Figure 10 depicts an example of such modification. We consider the case that the i-th pitch joint reaches the limit angle. Let ψ_{L} be the limit angle and let $\psi_{i\mathrm{d}}$ be the target angle of the i-th pitch angle. In the case that $\psi_{i\mathrm{d}} > \psi_{\mathrm{L}}$, we design the i-th pitch angle to be $\psi_i = \psi_{\mathrm{L}}$ and tilt the i-th module forward by $\alpha = \psi_{i\mathrm{d}} - \psi_{\mathrm{L}}$. The values of ψ_{i-1} and ψ_{i-2} are then modified so that the $(i-2)$-th wheel continues to touch the tread surface. As a result, the robot can shift the connecting part while avoiding the joint limit. The part of the robot from the head to the i-th module temporarily moves forward while avoiding this joint limit. Note that success in stair climbing is not guaranteed because there is always the possibility that the part will come into contact with the stairs when it is temporarily moved forward.

REFERENCES

[1] G. Granosik, "Hypermobile Robots – the Survey," *J. of Intelligent and Robotic Systems*, vol.75, no.1, pp.147-169, 2014.

[2] H. Streich and O. Adria, "Software Approach for the Autonomous Inspection Robot MAKRO," *Proc. IEEE Int. Conf. on Robotics and Automatin*, pp.3411-3416, 2004.

[3] B. Klaassen and K. L. Paap, "GMD-SNAKE2: A Snake-Like Robot Driven by Wheels and a Method for Motion Control," *Proc. IEEE Int. Conf. on Robotics and Automation*, pp.3014-3019, 1999.

[4] A. A. Fjerdingen, P. Liljebäck, and A. A. Transeth, "A snake-like robot for internal inspection of complex pipe structures (PIKo)," *Proc. IEEE/RSJ Int. Conf. on Intelligent Robots and Systems*, pp.5665-5671, 2009.

[5] A. Kakogawa and S. Ma, "Design of a Multilink-articulated Wheeled Inspection Robot for Winding Pipelines: AIRO-II," *Proc. IEEE/RSJ Int. Conf. on Intelligent Robots and Systems*, pp.2115-2121, 2016.

[6] T. Kamegawa, T. Yamasaki, H. Igarashi, and F. Matsuno, "Development of The Snake-like Rescue Robot "KOHGA"," *Proc. IEEE Int. Conf. on Robotics and Automation*, pp.5081-5086, 2004.

[7] M. Arai, Y. Tanaka, S. Hirose, H. Kuwahara, and S. Tsukui, "Development of "Souryu-IV" and "Souryu-V:" Serially connected crawler vehicles for in-rubble searching operations," *J. of Field Robotics*, vol.25, issue 1, pp.31-65, 2008.

[8] L. Pfotzer, S. Klemm, A. Roennau, J. M. Zöllner, and R. Dillmann, "Autonomous Navigation for Reconfigurable Snake-Like Robots in Challenging, Unknown Environments," *Robotics and Autonomous Systems*, 2016. (DOI: 10.1016/j.robot.2016.11.010)

[9] J. Borenstein, M. Hansen, and A. Borrell, "The OmniTread OT-4 Serpentine Robot–Design and Performance," *J. of Field Robotics*, vol.24, no.7, pp.601-621, 2007.

[10] K. Kydd, S. Macrez, and P. Pourcel, "Autonomous Robot for Gas and Oil Sites," *SPE Offshore Europe Conf. and Exhibition*, Society of Petroleum Engineers, 2015.

[11] H. Yamada, S. Takaoka, and S. Hirose, "A snake-like robot for real-world inspection applications (the design and control of a practical active cord mechanism)," *Advanced Robotics*, vol.27, no.1, pp.47-60, 2013.

[12] K. Kouno, H. Yamada, and S. Hirose, "Development of Active-Joint Active-Wheel High Traversability Snake-Like Robot ACM-R4.2," *J. of Robotics and Mechatronics*, vol.25, no.3, pp.559-566, 2013.

[13] S. Hirose, E. F. Fukushima, and S. Tsukagoshi, "Basic Steering Control Methods for The Articulated Body Mobile Robot," *IEEE Control Systems Magazine*, vol.15, no.1, pp.5-14, 1995.

[14] H. Komura, H. Yamada, S. Hirose, G. Endo, and K. Suzumori, "Development of snake-like robot ACM-R8 with large and mono-tread wheel," *Advanced Robotics*, vol.29, no.17, pp.1081-1094, 2015.

[15] T. Kinugasa, T. Haji, K. Yoshida, H. Amano, R. Hayashi, K. Tokuda, and M. Iribe, "Development of Flexible Mono-Tread Mobile Track Using Rotational Joints," *J. Intelligent & Robotic Systems*, pp.1-16, 2016.

[16] W. R. Hutchison, B. J. Constantine, J. Borenstein, and J. Pratt, "Development of Control for a Serpentine Robot," *Proc. IEEE Int. Symp. on Computational Intelligence in Robotics and Automation*, pp.149-154, 2007.

[17] B. Murugendran, A. A. Transeth and S. A. Fjerdingen, "Modeling and path-following for a snake robot with active wheels," *IEEE/RSJ Int. Conf. on Intelligent Robots and Systems*, pp. 3643-3650, 2009.

[18] M. Tanaka, M. Nakajima, and K. Tanaka, "Smooth Control of an Articulated Mobile Robot with Switching Constraints," *Advanced Robotics*, vol.30, no.1, pp.29-40, 2016.

[19] M. Tanaka, K. Kon, and K. Tanaka, "Range-sensor-based Semiautonomous Whole-body Collision Avoidance of a Snake Robot," *IEEE Trans. on Control Systems Technology*, vol.23, no.5, pp.1927-1934, 2015.

[20] M. Tanaka and K. Tanaka, "Control of a Snake Robot for Ascending and Descending Steps," *IEEE Trans. on Robotics*, vol.31, no.2, pp.511-520, 2015.

[21] K. Kon, M. Tanaka, and K. Tanaka, "Mixed Integer Programming Based Semi-autonomous Step Climbing of a Snake Robot Considering Sensing Strategy," *IEEE Trans. on Control Systems Technology*, vol.24, no.1, pp.252-264, 2016.

[22] H. Tsukano, M. Tanaka, and F. Matsuno, "Control of a Snake Robot on a Cylindrical Surface Based on a Kinematic Model," *Proc. 9th IFAC Symposium on Robot Control*, pp.865-870, 2009.

[23] M. Tanaka and K. Tanaka, "Stair Climbing of an Articulated Mobile Robot via Sequential Shift," *2015 IEEE/SICE International Symposium on System Integration*, SuE1.3, pp.877-881, 2015.

[24] S. Hirose, Biologically Inspired Robots (Snake-like Locomotor and Manipulator), Oxford University Press, 1987.

[25] A. Transeth, R. Leine, C. Glocker, K. Pettersen, and P. Liljebäck, "Snake Robot Obstacle-Aided Locomotion: Modeling, Simulations, and Experiments," *IEEE Trans. on Robotics*, vol.24, no.1, pp.88-104, 2008.

[26] T. Kamegawa, T. Watanabe, S. Yuan, and A. Gofuku, "Reactive motion for a snake-like robot in a crowded space," *Int. Electronic J. of Nuclear Safety and Simulation*, vol.6, no.2, pp.109-115, 2015.
[27] T. Kano, R. Yoshizawa, and A. Ishiguro, "TEGOTAE-Based Control Scheme for Snake-Like Robots That Enables Scaffold-Based Locomotion," *Biomimetic and Biohybrid Systems*, pp.454-458, 2016.
[28] X. Wu and S. Ma, "Neurally Controlled Steering for Collision-Free Behavior of a Snake Robot," *IEEE Trans. on Control Systems Technology*, vol.21, no.6, pp.2443-2449, 2013.
[29] D. Rollinson and H. Choset, "Gait-Based Compliant Control for Snake Robots," *Proc. IEEE Int. Conf. on Robotics and Automation*, pp.5123-5128, 2013.
[30] D. Rollinson and H. Choset, "Pipe Network Locomotion with a Snake Robot," *J. of Field Robotics*, vol. 33, no. 3, pp. 322-336, 2016.
[31] M. Vespignani, K. Melo, M. Mutlu, and A. J. Ijspeert, "Compliant snake robot locomotion on horizontal pipes," *Proc. IEEE Int. Symp. Safety, Security Rescue Robotics*, 2015.
[32] M. Travers, J. Whitman, P. Schiebel, D. Goldman, and H. Choset, "Shape-Based Compliance in Locomotion," *Proc. Robotics: Science and Systems*, 2016.
[33] H. Yamada and S. Hirose, "Study of Active Cord Mechanism – Approximations to Continuous Curves of a Multi-joint Body–," J. of the Robotics Society of Japan, vol.26, no.1, pp. 110-120, 2008 (in Japanese with English summary).
[34] H. Hasegawa, Y. Suzuki, A. Ming, K. Koyama, M. Ishikawa, and M. Shimojo, "Net-Structure Proximity Sensor: High-Speed and Free-Form Sensor With Analog Computing Circuit," *IEEE/ASME Trans. on Mechatronics*, vol. 20, no. 6, pp.3232-3241, 2015.
[35] A. Jacoff, "Standard Test Methods For Response Robots," *ASTM Int. Standards Committee on Homeland Security Applications; Operational Equipment; Robots (E54.08.01)*, 2016.
[36] ISO, "Safety of machinery - Permanent means of access to machinery - Part 3: Stairs, stepladders and guard-rails," ISO 14122-3, 2001.
[37] M. Tanaka and K. Tanaka, "Shape Control of a Snake Robot with Joint Limit and Self-collision Avoidance," *IEEE Trans. on Control Systems Technology*, Accepted. DOI: 10.1109/TCST.2016.2614832

Motoyasu Tanaka (S'05 - M'12) received his B.Eng., M.Eng., and Ph.D. degrees in Engineering from the Department of Mechanical Engineering and Intelligent Systems at the University of Electro-Communications, Japan in 2005, 2007, and 2009, respectively. From 2009 to 2012, he worked at Canon, Inc., Tokyo, Japan. He is currently an Associate Professor in the Department of Mechanical and Intelligent Systems Engineering at the University of Electro-Communications. His research interests include biologically inspired robotics and dynamics-based nonlinear control. He received the IEEE Robotics and Automation Society Japan Chapter Young Award from the IEEE Robotics and Automation Society Japan Chapter in 2006, and the Best Poster Award at SWARM2015: The First International Symposium on Swarm Behavior and Bio-Inspired Robotics in 2015.

Mizuki Nakajima received his B.Eng. and M.Eng. degrees in Engineering from the Department of Mechanical Engineering and Intelligent Systems at the University of Electro-Communications, Tokyo, Japan in 2014, and 2016, respectively. He is currently a Ph. D. candidate in the Department of Mechanical and Intelligent Systems Engineering at the University of Electro-Communications. His research interests include the development and control of snake robots.

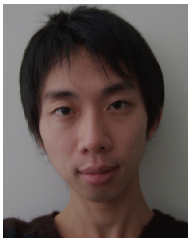

Yosuke Suzuki (M'17) received the B.Eng., M.Eng. and Dr.Eng. degrees from Tokyo Institute of Technology, Japan, in 2005, 2007 and 2010, respectively. He is currently an Assistant Professor with the Faculty of Mechanical Engineering, Institute of Science and Engineering, Kanazawa University, Japan. His research interests include modular robots, tactile and proximity sensors, and robotic grasping.

Kazuo Tanaka (S'87 - M'91 - SM'09 - F'14) received his B.S. and M.S. degrees in Electrical Engineering from Hosei University, Tokyo, Japan, in 1985 and 1987, respectively, and his Ph.D. in Systems Science from Tokyo Institute of Technology, Tokyo, Japan, in 1990. He is currently a Professor in the Department of Mechanical and Intelligent Systems Engineering at the University of Electro-Communications, Tokyo, Japan. He was a visiting computer scientist at the University of North Carolina at Chapel Hill in 1992 and 1993.

He received the Best Young Researcher Award from the Japan Society for Fuzzy Theory and Systems in 1990, the Outstanding Paper Award at the 1990 Annual NAFIPS Meeting in Toronto, ON, Canada in 1990, the Outstanding Paper Award at the Joint Hungarian-Japanese Symposium on Fuzzy Systems and Applications in Budapest, Hungary in 1991, and the Best Young Researcher Award from the Japan Society for Mechanical Engineering in 1994. He also received the Outstanding Book Award from the Japan Society for Fuzzy Theory and Systems in 1995, the 1999 IFAC World Congress Best Poster Paper Prize in 1999, the 2000 IEEE Transactions on Fuzzy Systems Outstanding Paper Award in 2000, and the Best Paper Selection at 2005 American Control Conference in Portland, OR in 2005. His research interests include intelligent systems and control, nonlinear systems control, robotics, brain–machine interfaces, and their applications. He is currently serving as an Associate Editor for Automatica and for IEEE Transactions on Fuzzy Systems, and is on the IEEE Control Systems Society Conference Editorial Board. He is the author of two books and coauthor of 17 books. Recently, he co-authored (with Hua O. Wang) the book Fuzzy Control Systems Design and Analysis: A Linear Matrix Inequality Approach (Wiley-Interscience, 2001).

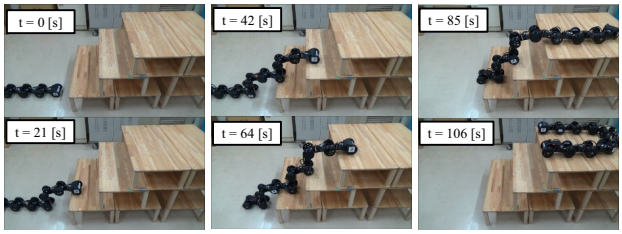

(a) Climbing up stairs, where $h_1 = 0.25$, $h_2 = 0.25$, $h_3 = 0.22$, $d_1 = 0.3$, and $d_2 = 0.27$.

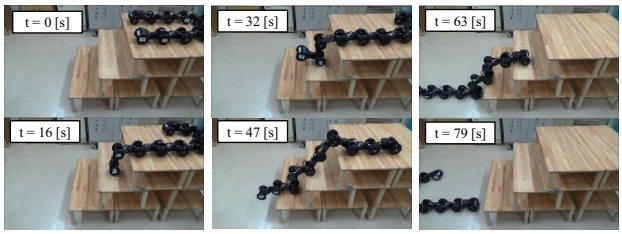

(b) Climbing down stairs, where $h_1 = 0.25$, $h_2 = 0.25$, $h_3 = 0.22$, $d_1 = 0.3$, and $d_2 = 0.27$.

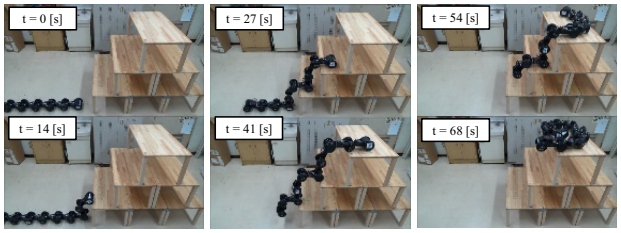

(c) Climbing up steep stairs, where $d_j = 0.25$, $h_j = 0.35$, and the rise/tread combination is 54.5°.

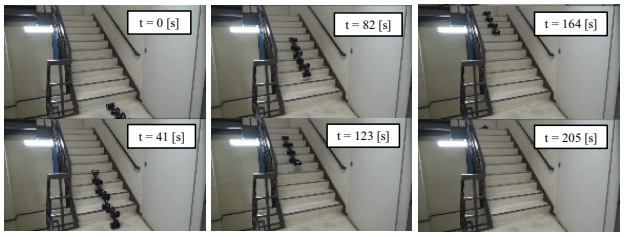

(d) Climbing up actual stairs, where $d_j = 0.255$ and $h_j = 0.185$.

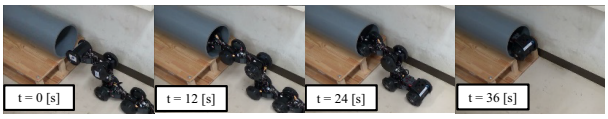

(e) Entering a pipe (pipe inner diameter: 194 mm).

Fig. 9. Photographs of the robot using the semiautonomous stair climbing method.

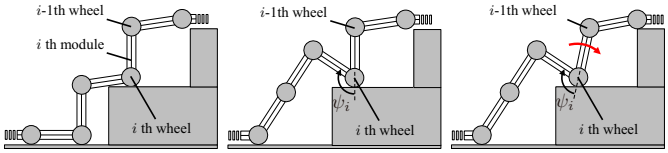

(a) (b) (c)

Fig. 10. Joint limit avoidance. (a) Before the shift, (b) during shifting, and (c) during shifting while avoiding the joint limit.